NEARSHORE COASTAL MAPPING

M-10

By Fabian C. Polcyn, Environmental Research Institute of Michigan, Ann Arbor, Michigan, and David R. Lyzenga, Environmental Research Institute of Michigan, Ann Arbor, Michigan

ABSTRACT

Two test sites of different water quality and bottom topography have been used to test for maximum water depth penetration using the Skylab S-192 MSS for measurement of nearshore coastal bathymetry. Sites under investigation lie along the Lake Michigan coastline where littoral transport acts to erode sand bluffs and endangers developments along 1,200 miles of shore, and on the west coast of Puerto Rico where unreliable shoal location and depth information constitutes a safety hazard to navigation.

Recent collisions of oil carrying supertankers with shallow obstructions highlight the need for an up-dating of world navigation charts especially in well traveled zones.

The S-192 and S-190A and B provide data on underwater features because of water transparency in the blue/green portion of the spectrum. Depth to 20 meters have been measured with the S-192 in the Puerto Rico test site. The S-190B photography with its improved spatial resolution clearly delineates the triple sand bar topography in the Lake Michigan test site.

Several processing techniques have been employed to test for maximum depth measurement with least error. The results are useful for helping to determine an optimum spectral bandwidth for future space sensors that will increase depth measurements for different water attenuation conditions where a bottom reflection is detectable.

INTRODUCTION

The research reported here is an outgrowth and continuation of previous research projects carried out at the Environmental Research Institute of Michigan for the purpose of developing methods of extracting water-depth information from multispectral scanner data collected by aircraft and satellites [1-4]. In particular, Reference [4] describes three such methods which were successfully applied to LANDSAT-1 data from the Caribbean and Lake Michigan. The present paper describes the application of these methods to data collected by the Earth Resources Experiment Package (EREP) of the Skylab Program. In addition, this paper contains an examination of the accuracy of the results as compared with published navigational charts, and an analysis of the types and magnitudes of errors inherent in each computational method.

The application potential of this technique can be seen from the recent announcements of losses of valuable crude oil as a result of collision of supertankers in different shipping lanes around the world. In general, world navigation charts are not current due to length of time for ship collection of data and subsequent map making and the dynamic processes for shifting sand bars and creating new shoals after storms. Also charts contain notations of shoal areas that are not verified in their depth or their location is known only approximately. Space acquired data offers the potential for providing more up-to-date information for navigation purposes thereby helping to reduce losses to life and property.

METHOD DATA EXTRACTION

The data used in this research included the S-192 (multispectral scanner) and S-190 (photographic) products from all three Skylab missions. The locations and dates of the three principal data sets were:

Skylab 2, Pass 6: Southwestern Puerto Rico - June 9, 1973
Skylab 3, Pass 14: Central Lake Michigan - August 5, 1973
Skylab 4, Pass 54: Eastern Puerto Rico - November 30, 1973

Photographic products from several other passes were received, but were considered to be too cloudy to be useful for analysis. Data were received in the form of photographic transparencies (S-190A and B), magnetic tapes containing the S-192 scanner data, and screening films made from these tapes. Processing of the films included enlarging and printing by ERIM's photographic laboratory, and in some cases scanning portions of the films with a Jarrell-Ash densitometer. Magnetic tapes were first converted to ERIM format on the University of Michigan's IBM 370 computer, and subsequently processed on ERIM's IBM 7094 computer.

The end product of the digital processing is a computer generated map on which different symbols are printed corresponding to various ranges of water depth.

In this paper, a portion of the depth map for the western coast of Puerto Rico is presented. On the map, depths from 0-15 meters are indicated in 3 meter intervals by means of five symbols, a sixth symbol indicates depth from 15 to 20 meters, and a seventh symbol for depths greater than 20 meters. For a second test site in Lake Michigan, a transect perpendicular to the shoreline was made for both photographic data and S-192 CCT data. The transects are of general usefulness because of the parallel sand bar structure along the Michigan shoreline.

Three methods of extracting water depth from the multispectral data have been used in the research reported, the single channel method, the ratio method, and the optimum-decision-boundary method. The single channel method works best when uniform conditions prevails in bottom reflectivity and water absorption characteristics. The ratio method yields the smallest error due to changes in the bottom reflectivity or water quality, but is susceptible to errors due to noise or changes in the surface-reflected signals. By using two channels, quantitative measurement of depth is obtained at the expense of calculating depths to the maximum depth of the second channel which is less than the maximum depth from the best penetrating channel.

The optimum-decision-boundary technique is not limited in this way and gives the best results when two equally penetrating channels are used. The best method for any given application area depends on the data quality, channels available, and type of changes occurring in the scene.

For the single channel method, the depth z is

$$z = -\frac{1}{\alpha f} \ln \frac{L_b}{L_o}$$

where L_o = radiance at zero water depth

α = water attenuation coefficient

$f = \sec \theta + \sec \phi$

θ = scan angle (underwater)

ϕ = solar zenith angle (underwater)

L_b = bottom reflected signal

Calculation of errors with this method shows that the error due to bottom changes is independent of depth, the error due to water attenuation changes in proportion to depth, and the error due to noise or surface fluctuations increases exponentially with depth. Therefore, at large depths, the latter type of error is always predominant.

In the ratio method, the radiance is measured in two channels i and j and the water depth is calculated using the following equation:

$$z = \frac{1}{(\alpha_j - \alpha_i) f} \ln \left(\frac{L_{b_i}}{L_{o_i}} \frac{L_{o_j}}{L_{b_j}} \right)$$

where symbols are defined as before but for different spectral channels.

The advantage of this method is that in some cases, a pair of channels can be found in which the ratio of the bottom reflectivities remains constant throughout the scene, or that the changes due to absorption differences are nearly the same for all wavelengths.

In the optimum-decision-boundary method the depth is calculated by the following expression

$$z = \frac{1}{(\alpha_i^2 + \alpha_j^2) f} \left[\alpha_i \ln \frac{L_{b_i}}{L_{o_i}} + \alpha_j \ln \frac{L_{b_j}}{L_{o_j}} \right]$$

In some cases by choosing spectral channels where reflectivities are negatively correlated, the error due to changes in bottom reflectivity may be reduced.

In this method, the error due to noise or surface reflectance changes is smallest if the two attenuation coefficients are equal or nearly equal.

A total error comparison was conducted for the three methods used and the results are shown in Figure 1.

Assumed values for the comparison were

$$\rho_{bi} = .130, \ \rho_{bj} = .135, \ \Delta\rho_{bi} = .070, \ \Delta\rho_{bj} = .070$$

$$\alpha_i = .19 \ m^{-1}, \ \alpha_j = .38 \ m^{-1}, \ \Delta\alpha_i = .07 \ m^{-1}, \ \Delta\alpha_j = .06 \ m^{-1}$$

$$\frac{\Delta L_{bi}}{L_{oi}} = \frac{\Delta L_{bj}}{L_{oj}} = .05$$

The reflectance parameters were taken from measurements off the North Carolina coast. The attenuation coefficients represent a change from minimum coastal to mean coastal water [1] at .55 and .60 μm. The noise parameters are representative of raw Skylab data. This combination of parameters does not describe any actual data set processed. However, it serves to show the relative errors for each method of processing.

The smallest error at very shallow depths is obtained by the ratio method. However, the errors using this method increase very rapidly with depth. The smallest error over the largest range of depths is obtained by the optimum decision boundary method for this set of parameters. This conclusion is probably valid for most cases, unless the water surface is very smooth and the bottom variations are very large.

RESULTS

Puerto Rico - West Coast. - In September 1974 a set of data tapes was received for the June 9, 1973 pass over the western coast of Puerto Rico. This set contained all 22 channels, and the noise in some of the channels (notably band 2) was less than that on the first tape received. The new tapes also contained data from about 10 seconds earlier, thus including parts of the western coast of Puerto Rico. This was important because the data collected just before the large cloud bank over Puerto Rico contains much less low-frequency noise then the subsequent data (apparently the noise was caused by the high signal received over the clouds).

A test area was selected which included shallow water features (indicated as Escollo Negro on the Coast and Geodetic Survey Chart 901). A large part of the west coast is obscured by clouds and by a large dark plume extending outward from Mayaguez. This plume has been tentatively identified as industrial waste products (possibly including fish oil and/or molasses) from plants near Mayaguez. Within the designated area, the plume follows the deep water boundary quite closely and, therefore, does not greatly affect the depth chart.

Processing of this area began by selecting a set of points where depths were indicated on C&GS Chart 901. Data values in bands 2 and 3 at these points were then extracted from the tape. The deep water signal V_s was subtracted from each data value and the results plotted versus depth on semi-log paper (Figure 2). A linear regression analysis of this data yielded an attenuation coefficient of approximately 0.05 m^{-1} for both bands, in agreement with minimum oceanic values published in the Smithsonian Physical tables.

A digital depth chart was then produced for this area, using the optimum-decision-boundary technique with the input parameters generated by the foregoing analysis. This chart is shown in Figure 3, where the symbols correspond to the depth ranges in Table 1. The white area in the upper right-hand corner is the tip of Punta Guanajibo. A portion of Coast and Geodetic Survey Chart 901 covering the same area is reproduced as Figure 4.

Next, an accuracy check was made by comparing depth values calculated by the optimum-decision-boundary technique with values read from the C&GS Chart. Both sets of values are plotted along line 1450 in Figure 5. The root-mean-square difference between the calculated and chart values along this line is approximately 2.4 meters. Subsequently, a depth transect corresponding to line 1440 was also received from J.V.A. Trumball [5] of the U.S. Geological Survey. A portion of this transect is plotted, along with the calculated values, in Figure 6. The r.m.s. difference between the calculated and observed values along this line is approximately 3.8 meters.

The greatest difference between calculated and observed depths occurs in the narrow channel running through the Escollo Negro (at approximately point 384 in Figures 5 and 6). Neglecting the possibility that this channel has actually filled in since the depth measurements were made, the error here is probably due to slow time-response characteristics of the S-192 sensor. Calculated depths in the Canal de Guanajibo are also smaller than the measured values. This difference is perhaps due to an increased surface-reflectance signal due to nearby clouds. Other sources of error include changes in the surface-reflected signal due to sea-state conditions, and changes in water quality or bottom reflectance.

Errors due to changes in water quality or bottom reflectance can be minimized by the use of the ratio method [4], but only at the expense of increased error due to changes in the surface-reflected signal. For the present case, the minimum overall error was obtained by the use of the optimum-decision-boundary technique, chiefly because of the relatively poor data quality in the red band (band 5) which is used in the ratio method.

Experience with low-altitude aircraft data [1-3] has indicated that depth accuracies on the order of 10-20% can be obtained using the ratio method. For a test site on Lake Michigan [3], the r.m.s. difference between the actual depth and the calculated depth using

wavelength bands of .57-.62 μm and .62-.69 μm was approximately 2.4 feet, out of a maximum depth of 25 feet. These results were obtained with the M-7 aircraft scanner [6], which has a noise-equivalent radiance of approximately 0.12 mw cm^{-2} μm^{-1} in these bands. The data was also smoothed to further reduce noise.

Lake Michigan Shoreline. - Data tapes from Skylab-3 pass 14 over Lake Michigan were received at ERIM in October 1974. Data was taken over the eastern shore of Lake Michigan during this pass at 15:01:30 GMT on 5 August 1973. Skies were clear over the Michigan shoreline and the solar zenith angle was approximately 45°.

Very little shallow water is visible in the scene because of the rapid drop-off in water depth along the shoreline. A Jarrell Ash scanning densitometer was used on an enlargement of S-190B photographic transparency to confirm distances measured by the S-192 data.

The densitometer scan shows three peaks at locations corresponding very closely to the peaks in the S-192 data. Assuming these are sandbars, the water depth can be calculated at each sandbar if the water attenuation coefficient is known. Unfortunately, no ground truth data was collected at this time of the overflight. However, an estimate can be made by using the attenuation coefficient $\alpha = .055$ ft^{-1} reported by Brown et al. [3] for Lake Michigan water at the wavelengths corresponding to band 3. The equation relating signal to depth is:

$$V = V_s + V_o e^{-\alpha f z}$$

where V = signal at depth z in band 3

V_s = signal over deep water ($z = \infty$)

V_o = bottom-reflected signal at shoreline ($z = 0$)

α = water attenuation coefficient

$f = \sec\theta + \sec\phi$

θ = scan angle (underwater)

ϕ = solar zenith angle (underwater)

Using the observed values $V_s = 55$, $V_o = 15$, and $f = 2.42$, the depths calculated for each sandbar are 13.4 ft, 10.0 ft, and 8.3 ft, respectively.

No direct depth measurements were made in this area, but Lake Survey Chart 77 shows two sandbars south of Pentwater at distances of about 210 and 360 meters from shore. The depths are indicated as about 6 and 10 feet, respectively, in fair agreement with the calculated depths. No third sandbar is shown on the Lake Survey Chart, but its existence is possible since they are known to form and disappear quite rapidly due to wave action.

CONCLUSIONS

The examples discussed in this paper indicate that shallow water features can be located rapidly using space-acquired imagery. Photographs provide greater spatial resolution but multispectral scanner data is needed to distinguish underwater features from surface phenomena and to provide quantitative estimates of water depth.

Significant improvement in depth penetration and spatial resolution over LANDSAT-1 data has been noted in Skylab scanner and photographic data. Skylab sensors have better band location, bandwidth, and gain characteristics than LANDSAT-1. However, the Skylab scanner has been plagued with noise and poor response characteristics, which have in some cases rendered the data less useful than LANDSAT-1 data. Attempts to use ratio depth processing have been less successful with Skylab than with LANDSAT data because of the noise in band 5. Methods of reducing noise by smoothing are less successful because of the conical scan configuration. However, the striping problem in LANDSAT due to differences in calibration of the six sensors is not present in Skylab.

Coordination of data products and determination of orbital and sensor parameters has been more difficult with Skylab than with LANDSAT data. Despite these problems, however, Skylab has generated a large amount of useful data which could be exploited by the techniques reported here, to contribute to the general store of hydrographic information or solve specific problems where an up-to-date knowledge of shallow water bottom topography over a large area is needed.

REFERENCES

1. F. C. Polcyn and R. A. Rollin, "Remote Sensing Techniques for the Location and Measurement of Shallow-Water Features," Report No. 8973-10-P, Willow Run Laboratories, January 1969.

2. F. C. Polcyn, W. L. Brown, and I. J. Sattinger, "The Measurement of Water Depth by Remote Sensing Techniques," Report No. 8973-26-F, Willow Run Laboratories, October 1970.

3. W. L. Brown, F. C. Polcyn, A. N. Sellman, and S. R. Stewart, "Water Depth Measurement by Wave Refraction and Multispectral Techniques," Report No. 31650-31-T, Willow Run Laboratories, August 1971.

4. F. C. Polcyn and D. R. Lyzenga, "Remote Bathymetry and Shoal Detection with ERTS", Report No. 193300-51-F, Environmental Research Institute of Michigan, April 1975.

5. J. V. A. Trumball, personal communication, April 11, 1975.

6. P. G. Hasell, et al., "Michigan Experimental Multispectral Mapping System - A Description of the M7 Airborne Sensors and its Performance", Report No. 190900-10-T, Environmental Research Institute of Michigan, January 1974.

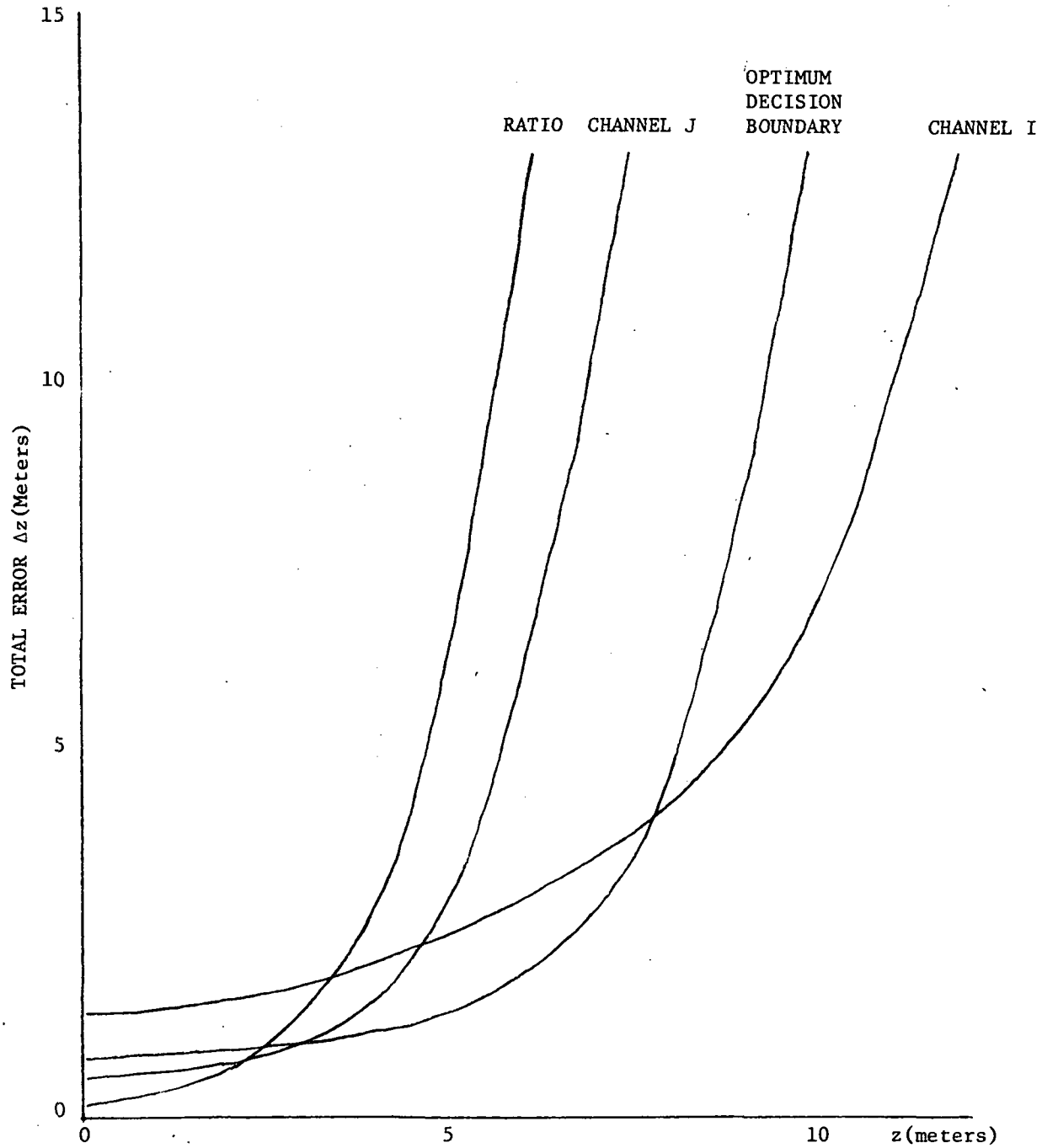

FIGURE 1. COMPARISON OF TOTAL ERROR

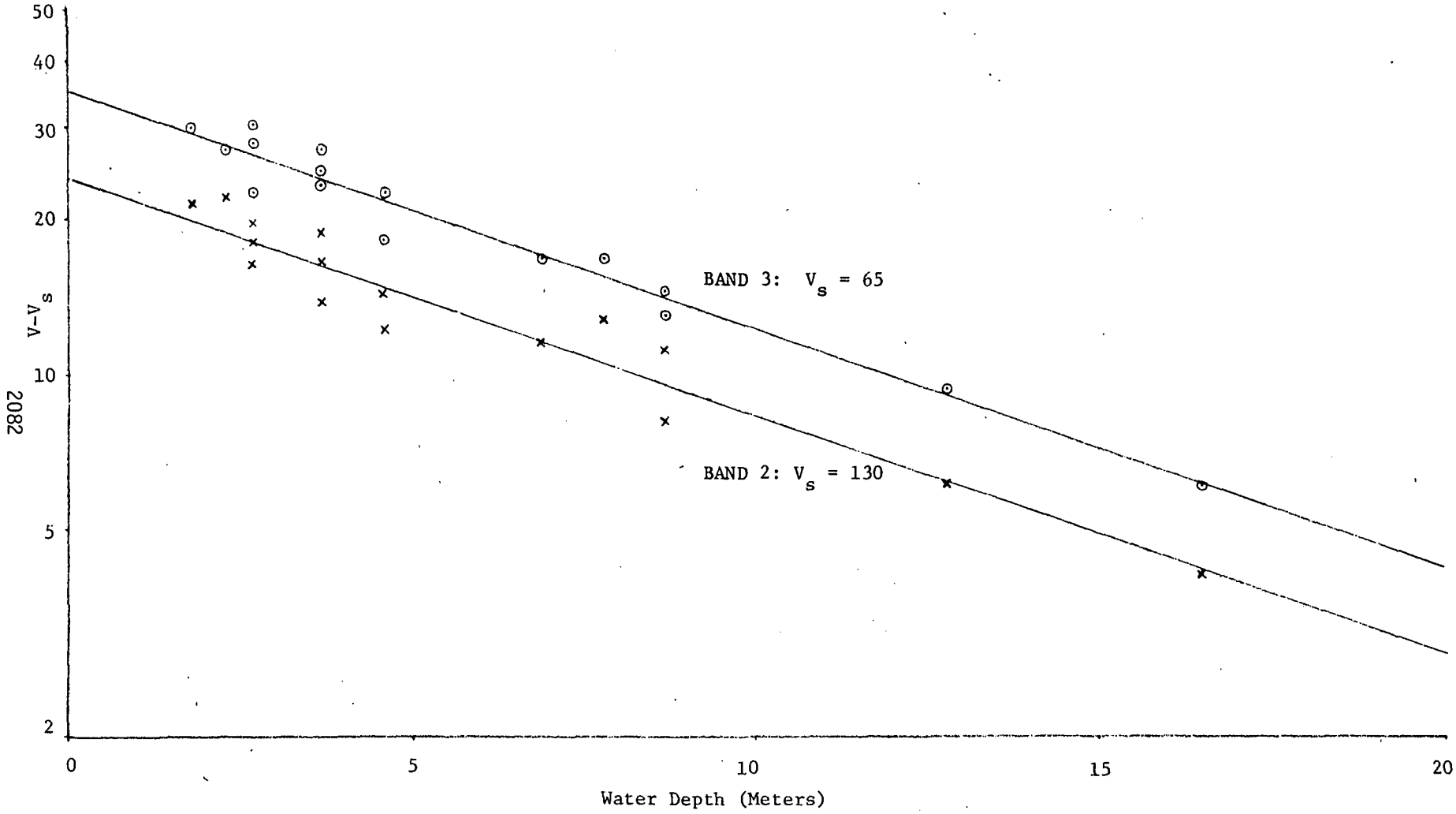

FIGURE 2. BAND 2 AND 3 SIGNALS VERSUS DEPTH, ESCOLLO NEGRO AREA.

TABLE I

METERS	SYMBOL
20-INF	⊠ = Blue
15-20	X = Blue
12-15	* = Blue
9-12	+ = Blue
6-9	* = Red
3-6	X = Red
0-3	⊠ = Red
LAND	

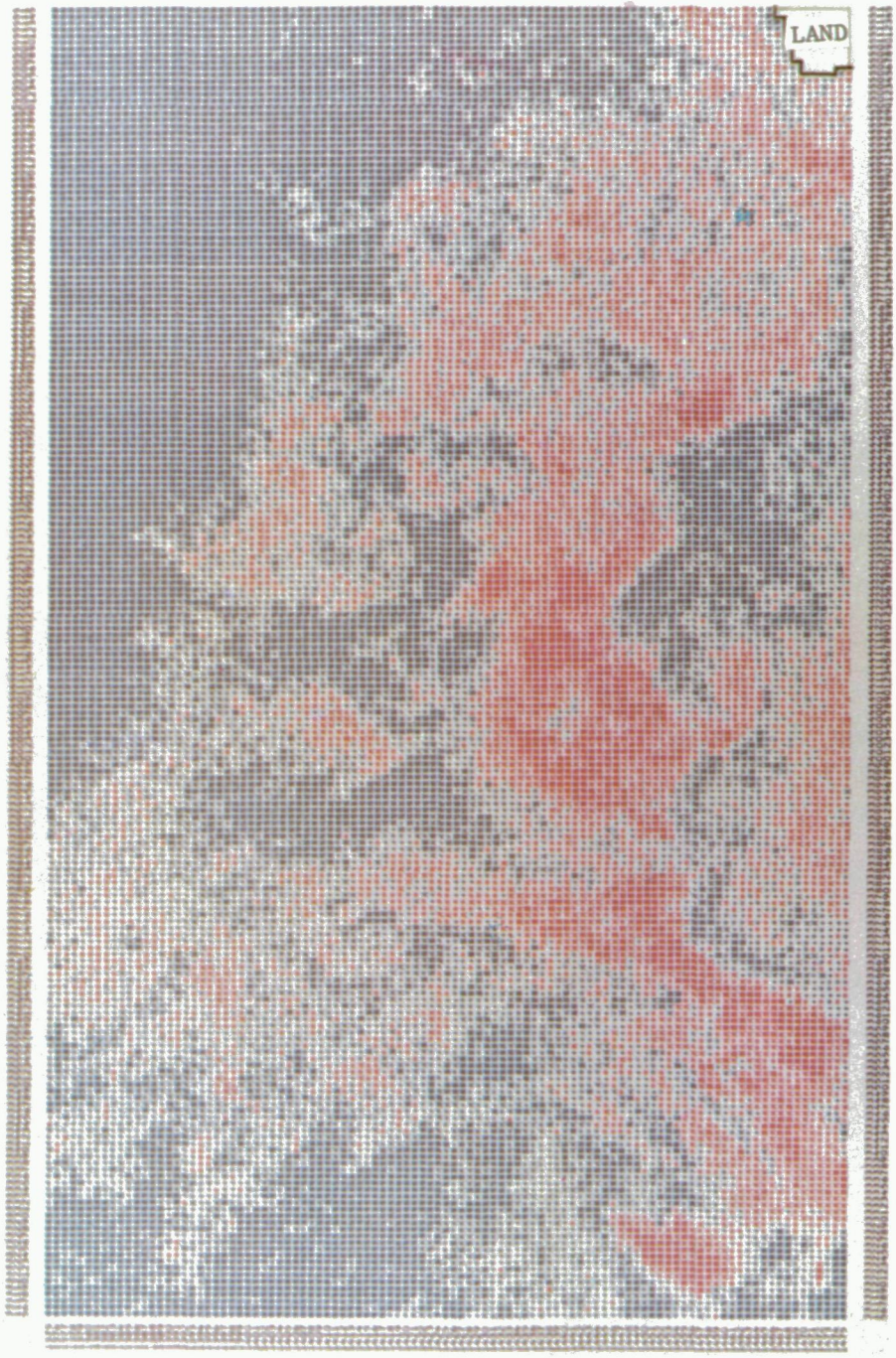

FIGURE 3. DIGITAL DEPTH CHART OF ESCOLLO NEGRO AREA

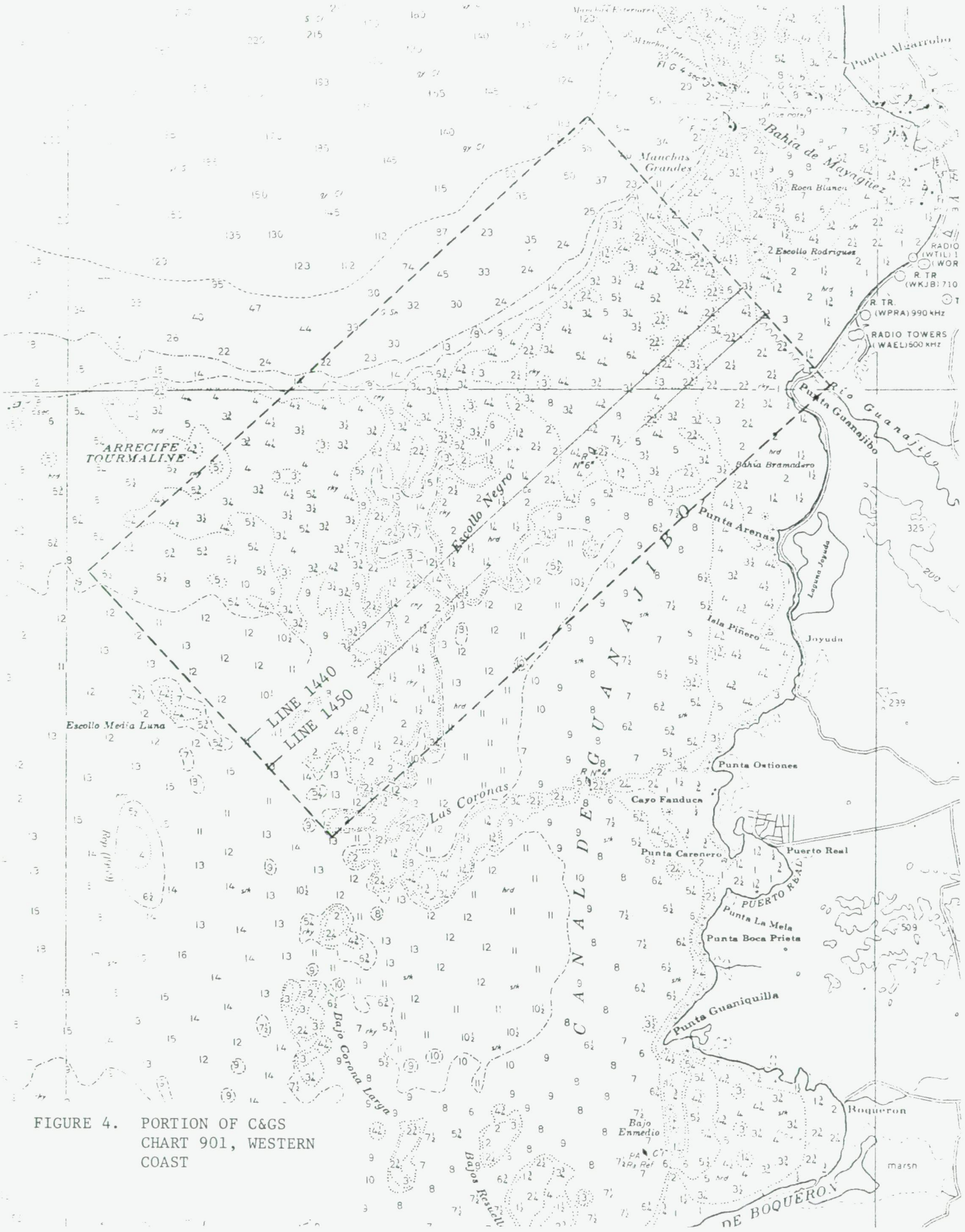

FIGURE 4. PORTION OF C&GS CHART 901, WESTERN COAST

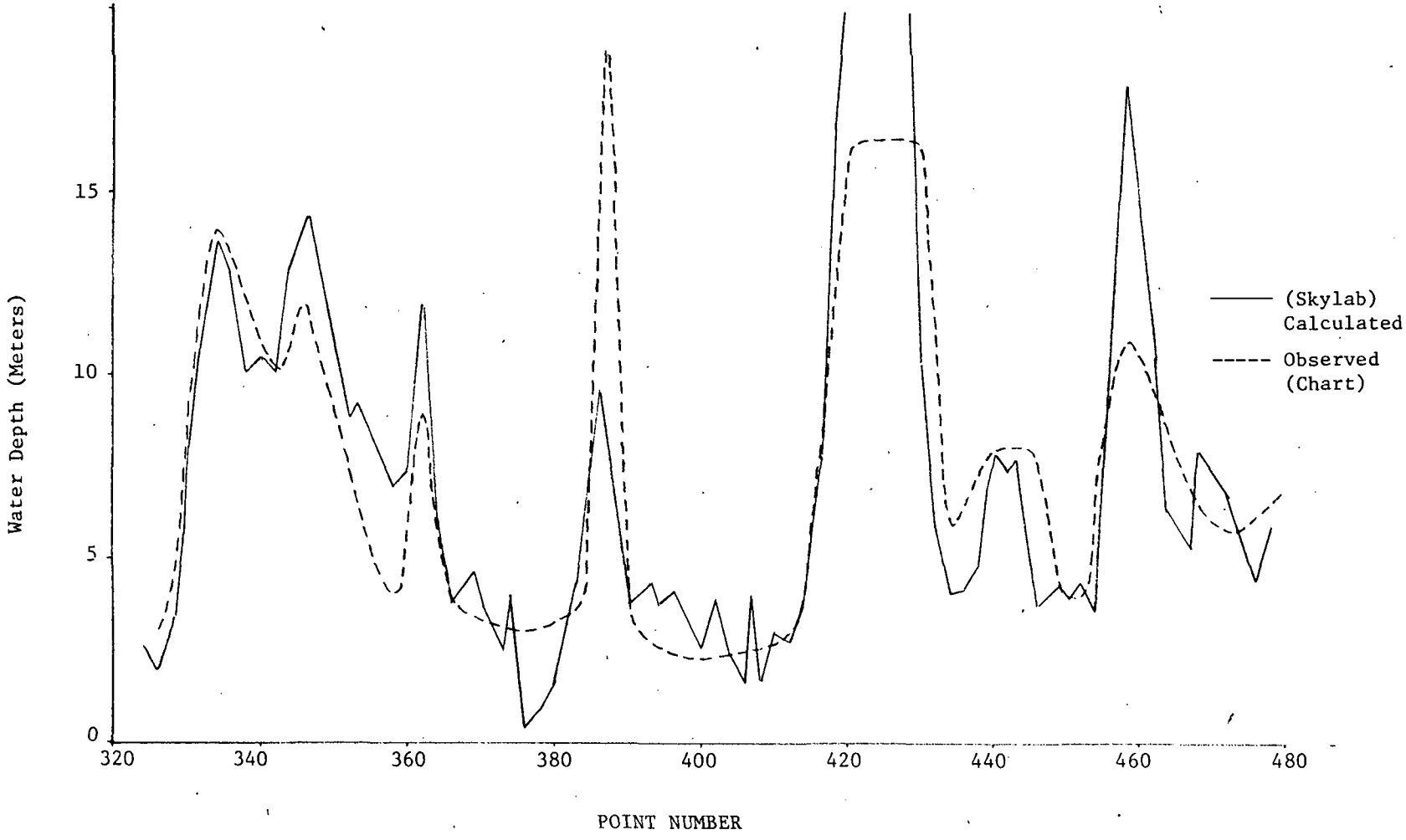

FIGURE 5. CALCULATED AND CHART DEPTHS ALONG LINE 1450

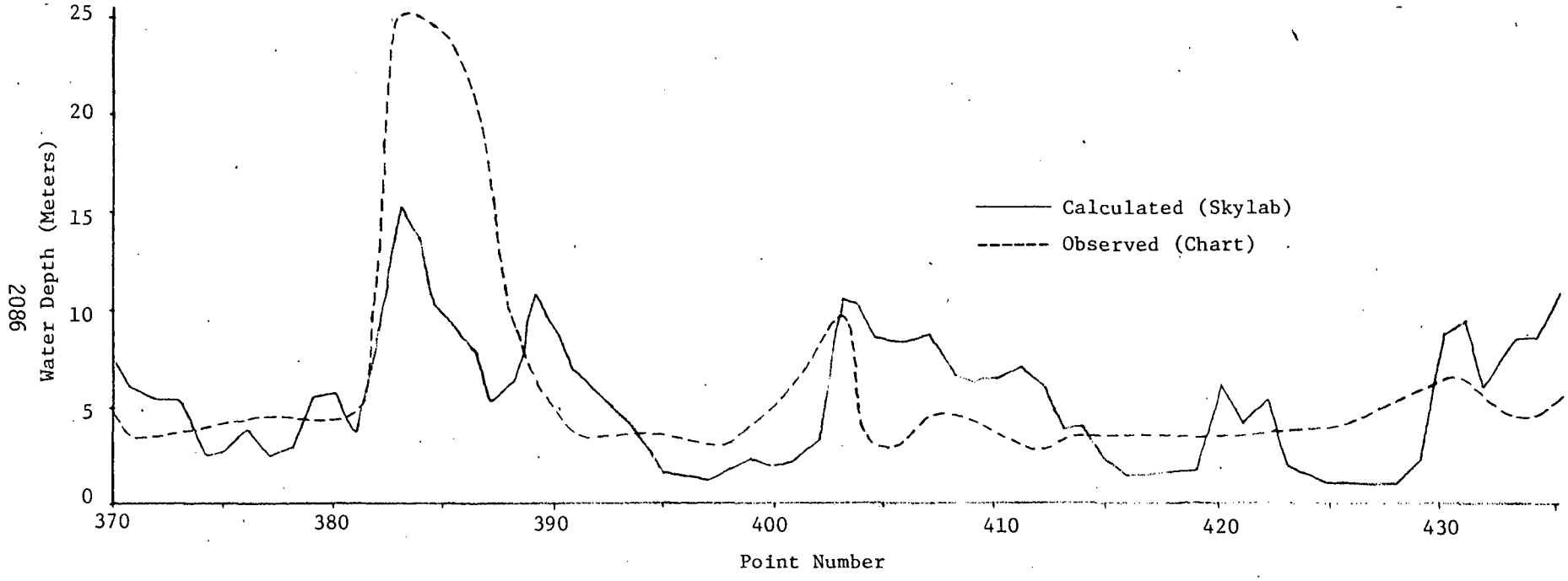

FIGURE 6. CALCULATED AND OBSERVED DEPTHS ALONG LINE 1440.